NURETH14-634

SUPERCRITICAL FLOW AND HEAT TRANSFER IN ADVANCED REACTORS

M. Corradini <u>Corradini@engr.wisc.edu</u>

Wisconsin Institute of Nuclear Systems, University of Wisconsin-Madison, WI, U.S.A.

Abstract

Nuclear power plants are currently operating throughout the world and supplying over one-sixth of the world's electricity. In spite of recent events in Japan, given the current rate of growth in electricity demand and the ever growing concerns for the environment, nuclear power remains a key technology to satisfy the need for electricity and other energy products if it can demonstrate (1) enhanced system reliability and safety, (2) minimal environmental impact via sustainable system designs, and (3) competitive economics. Since 2000, the United States in collaboration with the international community has begun research on the next generation of nuclear energy systems that can be made available to the market over the next couple of decades, and may offer significant advances toward these challenging goals. Near-term deployment of advanced water-cooled thermal reactors are being ordered or under construction. Beyond this next decade, there are future nuclear power systems (so-called Generation IV or GenIV) that require advances in materials, reactor physics and heat transfer to realize their potential. In particular, the use of supercritical fluids in GenIV nuclear systems has gained prominence. The focus of this paper is to summarize some of the key supercritical heat transfer topics that are being addressed to assure appropriate reliable design and operation of these advanced nuclear systems.

1. Introduction

Advanced water-cooled-reactor nuclear energy system concepts have been identified as part of the Generation IV International Roadmap evaluation [1] and associated research and development activities; i.e., involving industry groups, international laboratories, as well as academia from countries including Argentina, Brazil, Canada, France, Italy, Japan, Korea, Russia, Switzerland, the UK and the U.S. Leading water-cooled reactor designs can be categorized into two general groups:

- Advanced Boiling Water (BWR) & Pressurized Water Reactors (PWR)
- Longer-Term Advanced Water Reactors

The first group of advanced BWR and PWR systems can be represented by the AP1000 (Advanced Pressurized Water Reactor [2]) and the ESBWR (Economic Simplified Boiling Water Reactor [3]), while the Supercritical Water Reactor (SCWR [4]) is one example of the second grouping. Also small modular reactors have been proposed that can be manufactured in a factory setting and shipped as a completed unit to an approved power plant site. These systems have much simpler safety systems and can be built as modules (IRIS is an early design [5] but others have been proposed; e.g., NuScale [6]). For this review paper, the SCWR is of particular interest.

Advanced reactors have also been proposed that utilize different coolants than water and potentially may allow for more flexibility in operation, improved sustainability and minimizing by-product flows as well as providing the potential for higher outlet temperatures to allow for a wider range of process heat applications; e.g., high-temperature synthetic fuel production. Many

concepts were proposed as part of the GenIV roadmap process and the most promising designs can be grouped into three broad categories:

- Advanced Gas-Cooled Reactors for High Temperatures (PBMR, MHTGR, VHTR, GFR)
- Advanced Liquid-Metal Fast Reactors (LMR Sodium-cooled and Lead-alloy-cooled)
- Innovative concepts, non-traditional coolant or fuel designs (Molten salt reactor, MSR)

The first grouping of advanced gas-cooled reactors can be represented by the Next-Generation Nuclear Plant, NGNP (a High Temperature gas-cooled Reactor [7]) either with graphite pebbles or with prismatic graphite blocks as moderators. The second grouping can be represented by the integral sodium-cooled fast reactor [8] or the lead-cooled fast reactor, both providing high-temperature process heat with a low pressure cooling circuit. The final category is now being revisited with the MSR [9] a novel reactor design for very high-temperature applications [10].

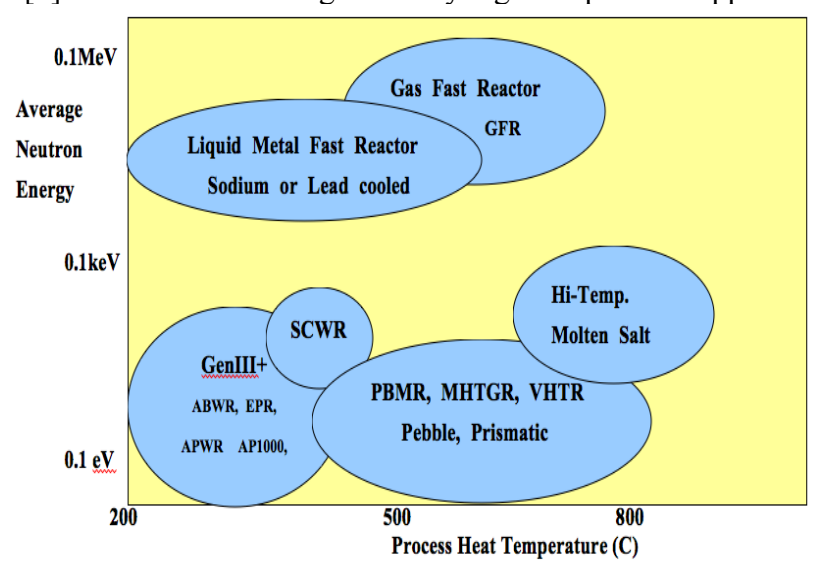


Figure 1: Concept Map of Advanced Nuclear Reactors

Consider Figure 1 as a way to represent these advanced reactor concepts, with the average neutron energy and process heat temperature as the key variables. If one considers the nuclear reactor as the heat source for a heat engine then the process heat temperature exiting the reactor is indicative of its ability to efficiently produce electricity (via a Rankine cycle or Brayton cycle), or to be used for producing a variety of energy products from process heat. In addition, the nuclear reactor average neutron energy is an important parameter since it controls the ability of the device to transmute fertile fuel, burn fissile fuel and burn long-lived radioactive actinides. Supercritical fluids is being considered for heat transfer in these advanced reactors for various purposes. In the SCWR, water is the moderator and coolant within the reactor core. For NGNP, LMR or MSR concepts, supercritical carbon-dioxide (SCO₂) is an intermediate transport fluid.

2.0 Supercritical Flow and Heat Transfer Investigations

In terms of heat transfer, fluids at supercritical pressures present interesting challenges. Even though no phase change takes place, at a given supercritical pressure strong variations in thermophysical properties occur over a small range of temperatures in the vicinity of the pseudo-critical point. These rapid variations have a significant effect on heat transfer behavior, and, depending

on heat flux and mass flow conditions, can cause either enhancement or deterioration relative to normal single-phase heat transfer [11]. The prediction of deteriorated conditions for the SCWR reactor design concept is particularly important, as very high local cladding temperatures are possible, which could lead to damage. Thus, in recent years a significant effort has been made to develop and improve heat transfer correlations for supercritical fluids, and continues [12-15].

2.1 Supercritical Water Heat Transfer Scaling and Experimental Investigations
Experimental studies with supercritical water are essential to continuing this effort for the SCWR reactor concept, in Asia and Europe. However, due to the high pressure (>220 bar) and temperatures (>374°C) required, such experiments are technically challenging and costly. Reproducing the conditions expected to be prototypic of the SCWR presents an even greater challenge, as operating pressures and temperatures are expected to be as high as 250 bar and 500-550°C, respectively [4]. The UW heat transfer flow loop has been used for supercritical water (SCW) experiments [11] and is now being modified to perform similar tests with SCO₂ [12]. Scaling of the appropriate conditions in SCO₂ can be determined by conserving key non-dimensional parameters from the SCW tests. The predicted heat transfer in the SCO₂ can be compared to measured data to evaluate the validity of the scaling method. As a secondary basis for validation, we are also using the FLUENT CFD tool for these scaled SCO₂ conditions and are comparing the simulations to the SCW experiments, which demonstrate good agreement with optically-measured turbulence data.

The scaling method adopted by Zwolinski et al [12] was based on discussions with Prof. Jackson and using a proposed non-dimensional temperature ratio. In general, a series of non-dimensional quantities are preserved; i.e., the length scale based on hydraulic diameter, the reduced pressure (P/P_c) , the Reynolds number, a proposed reduced temperature (T/T_{SC}) and the Nusselt number (or equivalently the heat fluxes). Normally a reduced temperature is used near critical pressures.

The SCW experiments conducted by Licht [11] covered a range of flow conditions in both circular-annular and square-annular geometry in the vertical upward flow configuration. Heat flux, mass flux, and bulk temperature were varied to cover the transition, forced, and mixed convection flow regimes in order to observe heat transfer enhancement, and deterioration brought on by buoyancy effects. The conditions considered are summarized in Table 1 below.

Table 1.	Conditions 1	n SCW	and S	caled to	sımılar	SCO_2	l'est (Conditions

Supercritical W	ater		Supercritical Carbon Dioxide			
Bulk	Mass Flux	Heat Flux	Bulk	Mass Flux	Heat Flux	
Temperature	[kg/m2-s]	[kW/m2]	Temperature	[kg/m2-s]	[kW/m2]	
[C]			[C]			
300	315, 1000	0, 220, 440	-4	400, 1270	0, 22, 43	
340	315, 1000	220, 440	15	345, 1095	20, 40	
370	315, 1000	220, 440	30	300, 950	18, 36	
380	315, 1000	220, 440	35	280, 890	16, 32	
397	315, 1000	220, 440	42	250, 780	18, 36	

All of the SCW tests in Table 1 were conducted at 250 bar, corresponding to 84 bar in SCO₂. Twenty-seven of the forty-seven SCW cases were replicated; water cases at bulk temperatures below 300°C cannot, regardless of scaling method, due to the excessively low corresponding temperatures in SCO₂. This is again due to the difference in the relative location of the critical point with respect to the freezing temperature of carbon dioxide, making some tests impractical.

In the SCW experiments, we used FLUENT 6.3 to gain insight into the flow behavior in the boundary layer, verifying the simulation results through comparison to the local turbulence data collected in the square annular geometry. As detailed in [11], in general, for carefully chosen model parameters the simulations were found to agree quite well with measurements. In view of this, comparison of CFD predictions for SCW and SCO2 at scaled conditions is expected to offer credible insight into the viability of the scaling method as measured SCO2 data come available. In the present study, version 12 of the FLUENT software was used to simulate the scaled SCO2 tests. For consistency, the radial geometry was modeled the same way as in [11], with a full-scale 1/8th section with symmetry boundaries on the non-wall edges (Figure 1). For all calculations, the Reynolds stress method (RSM) was used to resolve the turbulence information. Validity of comparison to the measured SCW data was confirmed in that no noticeable change was observed between the SCW simulation results in [11] and these results without deterioration.

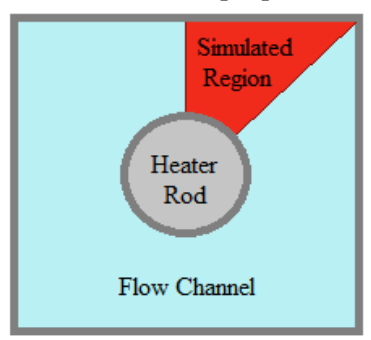


Figure 1. Schematic of the radial computational domain

In total, seven pairs of SCW - SCO₂ cases were simulated to observe the effects of mass flux, heat flux, and bulk temperature on the turbulence behaviour for both fluids. These tests are summarized in Table 2. Again, all SCW cases were at 250 bar, and all SCO₂ cases at 84 bar.

	Supe	rcritical Wate	r	Supercritical Carbon Dioxide			
Case	Bulk	Mass Flux	Heat Flux	Bulk	Mass Flux	Heat Flux	
Number	Temperature	$[kg/m^2-s]$	$[kW/m^2]$	Temperature	$[kg/m^2-s]$	$[kW/m^2]$	
	[C]			[C]			
1	300	985	0	-3	1310	0	
2	300	985	220	-3	1310	22	
3	300	985	440	-3	1310	43	
4	370	985	220	30	940	19	
5	397	985	440	42	775	50	
6	300	285	220	-4	380	22	
7	397	285	440	42	780	36	

Table 2. SCW and scaled SCO₂ case pairs simulated in FLUENT

The results compared favorably primarily on the basis of their agreement with the four main turbulence parameters [12]. These are the normalized axial velocity, axial and radial turbulent intensity, and Reynolds stress. The FLUENT predictions in scaled SCO₂ agreed almost exactly with the analogous results in SCW, regardless of mass flux, heat flux, and bulk temperature.

2.2 Supercritical Carbon-Dioxide Heat Transfer Experiments

Closed-loop Brayton cycles using supercritical carbon dioxide (SCO₂) have been gaining interest recently for use in high-temperature power generation applications including High-temperature Gas-cooled reactors (e.g., NGNP) and Sodium-cooled fast reactors. Compared to Rankine cycles SCO₂ Brayton cycles offer improved thermal efficiency and the potential for decreased capital costs due to a reduction in equipment size and complexity. Compact printed-circuit heat exchangers (PCHE) are being considered as part of several SCO₂ designs to further reduce equipment size with increased energy density. Plans include a pre-cooler/regenerator operating near the carbon-dioxide pseudo-critical point to benefit from large variations in thermo-physical properties. But further work is needed to validate correlations for heat transfer and pressure-drop characteristics of SCO₂ flows in candidate PCHE designs for a range of operating conditions.

Our work has focused on the heat transfer and pressure drop behavior of miniature channels using carbon dioxide at supercritical pressure. A zig-zag plate geometry based on the cold-fluid side of a 'Heatric' PCHE was tested in a horizontal orientation in the cooling mode for bulk temperatures from 20-65C at 7.5-8.1 MPa and a mass flux of 326 kg/m²-sec. Heat transfer coefficients and bulk temperatures are calculated from measured local wall temperatures and local heat fluxes as we use computational model to analyze these data.

A test facility has been developed at UW Madison to investigate the heat transfer and pressure drop characteristics of a variety of PCHE channel geometries, and has been used previously [13] to gather data on straight semi-circular millimeter-scale channels in both heating and cooling modes, and in horizontal, vertical upward, and vertical downward flow for a variety of pressures and mass fluxes. In current work [14], the test facility was used with a horizontal zig-zag plate geometry modeled after that found on the cold-side of a Heatric PCHE to investigate the heat transfer and pressure drop characteristics of SCO₂ in cooling mode flow as in a precooler unit.

The experimental facility used, which has been described previously [13], consists primarily of a recirculation loop and a test section loop. In the recirculation loop a throttle valve is set to divert flow through the test section, to maintain a constant mass flow rate through the channels. The mass flow rate diverted through the test section loop is monitored with a Coriolis flow meter. The flow then passes through a custom-built heater coil before being cooled in the test section and returning to the recirculation loop. The testing capabilities of the experimental facility pertaining to heat transfer and pressure drop studies of SCO₂ are summarized below.

Table 3. A Summary of Flow Conditions Possible in the UW Test Facility

Experimental Facility Capabilities							
	Pressure [MPa]	Reynolds # [-]	Mass Flux [kg/m ² -s]	T _{INLET} [C]			
Low	7.38	5000	300	15			
High	20	100000	1200	150			

The test section (Fig. 2) consists of two 316 stainless steel plates representative of printed-circuit heat exchangers with one plate flat and the other plate chemically etched (Microphoto Inc.) with a variety of channel geometries. Each plate has a flow channel length of 0.5m, with plenums milled at both the inlet and outlet to the flow channels. Two type-E thermocouples calibrated against a NIST-traceable RTD are located in each plenum to measure inlet and outlet temperatures of the S-CO2 flow, as well as pressure ports for inlet pressure measurement and to measure the differential pressure across the test section. The flow area is subdivided into 10 subsections with aluminum cooling blocks bolted to each side of the plates and thermocouples implanted in the center of each sub-section of each plate just above the flow channels in 1mm holes. Each cooling block is provided with a flow of cooling water by a portable cooling bath with the volumetric flow rate into each cooling block measured by individual flow meters and the inlet and outlet temperatures of each cooling block measured with type E thermocouples.

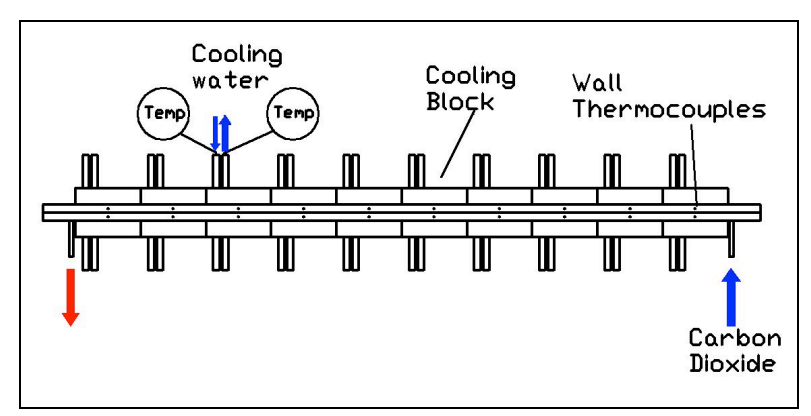


Figure 2. Measurements available from the test section include inlet and outlet temperatures of the SCO_2 flow and each cooling block, mass flow rate of the SCO_2 and volumetric flow rates of through each cooling block, and inlet and differential pressure of the SCO_2 flow through the test section.

The two plate geometries currently considered are a straight-channel geometry with a semi-circular cross section presented previously by Kruizenga [13], and a zig-zag geometry representative of the cold-side flow path in a HeatricTM heat exchanger. The semi-circular geometry consists of nine 1.9 [mm] diameter channels, while Figure 3 describes the geometry of the cold-side zig-zag flow path consisting similarly of nine zig-zag flow channels.

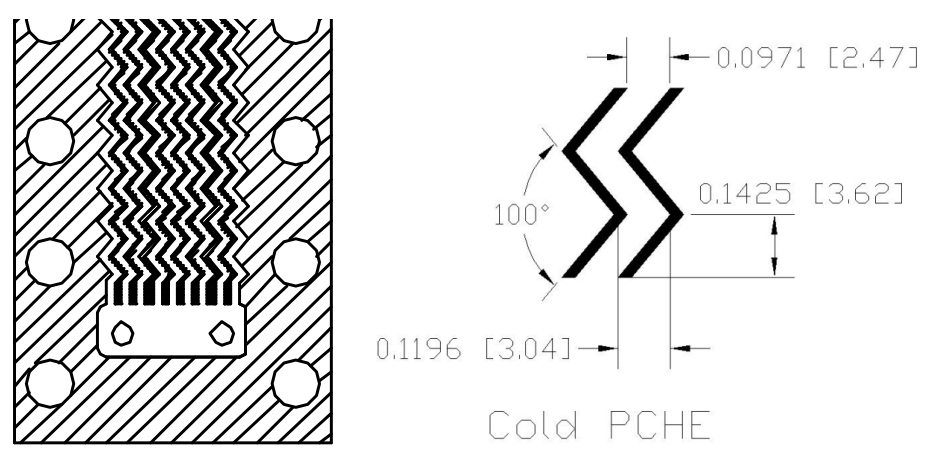


Figure 3. Diagram of the cold-side zig-zag channel geometry [13].

The key geometric parameters of each plate are summarized in Table 4, where L is the channel length parallel to the net flow direction, d_{hyd} is the hydraulic diameter of one channel, z is the distance from the channel wall to the wall thermocouples, A is the area available for conduction between the channel wall and the wall thermocouples, A_S is the surface area of the channels in one sub-section, $A_{channels}$ is the cross-sectional area of the channels perpendicular to the net flow direction, $A_{manifold}$ is the cross-sectional area of the manifold in a plane parallel to the cross sectional area of the channels, and RR is the relative roughness of the channel surface. These are used in our analysis of pressure drop and heat transfer coefficients (see details in Ref. 13 – 14).

Table 4. Test Plate Channel Geometric Parameters								
	L [m]	d _{hyd} [m]	z [m]	$A [m^2]$	$A_{S} [m^2]$	A _{channels} [m ²]	A _{manifold} [m ²]	RR [-]
Straight Semi- circular	0.5	1.161e-3	3.175e-3	1.794e-3	2.198e-3	12.76e-6	95.23e-6	6.4e-3
Cold-side Zig-Zag	0.5	1.161e-3	3.175e-3	1.794e-3	2.870e-3	12.76e-6	95.23e-6	6.4e-3

The zig-zag mini-channels are compared to previous straight-channel data at 8.1 MPa case. Figure 4 shows a comparison of two datasets with uncertainty bars removed for clarity, although it should be noted that the uncertainty in the straight-channel data is approximately five times smaller near the pseudo-critical temperature the uncertainty in the cold-side zig-zag channel data, and negligible farther away from the pseudo-critical temperature. It can clearly be seen that the change in channel geometry increases the heat transfer from the carbon dioxide by almost three times for all temperatures, but shows a very similar trend to the straight-channel data with the Nusselt number rising as the bulk temperature approaches the pseudo-critical temperature, reaching a maximum just before the pseudo-critical temperature as the temperature of the viscous sub-layer passes through the pseudo-critical point, and falls sharply after that point.

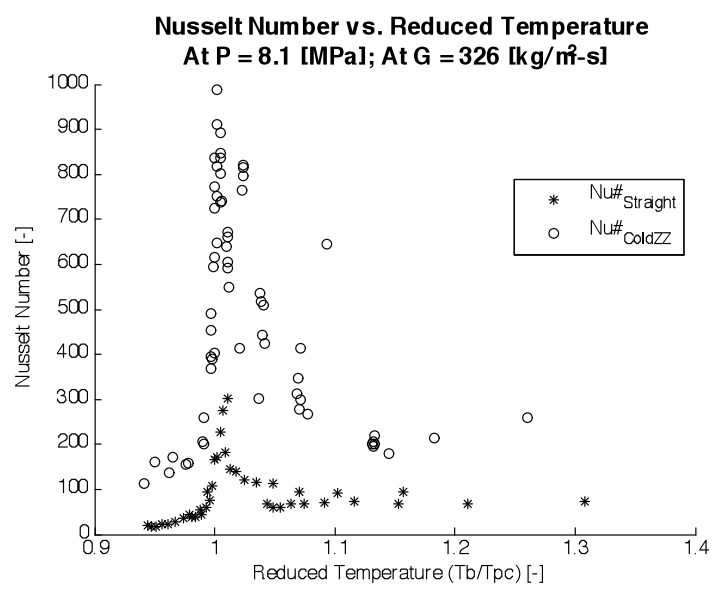


Figure 4 Nusselt number vs. temperature ratio (Tb/Tpc) for both the zig-zag and straight channels. The measured total pressure drop across both the straight channels and cold-side zig-zag channels is shown in Figure 5, representing data from both pressure values and at two different mass fluxes. As shown previously by Kruizenga [13], the pressure drop across the straight channel is dominated by frictional pressure loss and is well-predicted by typical correlations

once local and acceleration components of the pressure drop, constant with Reynolds number, are accounted for. It can be clearly seen however that pressure drop in the cold-side zig-zag channel geometry does not scale similarly with increasing Reynolds number due to the additional form loss associated with the bends in zig-zag channels, which scale with Reynolds number.

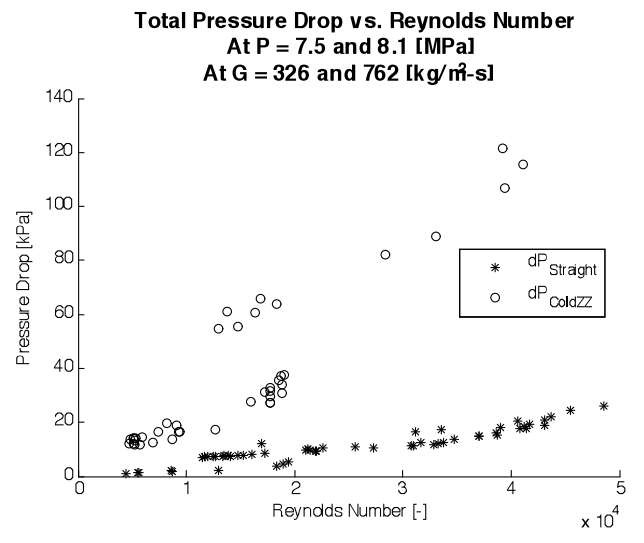


Figure 5. Total pressure drop vs. Reynolds number for both the zig-zag and straight channels

2.3 Supercritical Carbon-Dioxide Heat Transfer Analysis

To better understand these SCO₂ data [13-14], we have begun numerical simulations of the flow characteristics within printed circuit heat exchangers (PCHEs) with zigzag channel geometries. The channels are modeled in their actual semi-circular shape using 3-dimensional computational fluid dynamics (CFD) simulations. These studies are being focused on investigation of the accuracy of the numerical simulations versus the existing experimental data for future designs.

The computational fluid dynamics (CFD) work was performed using the commercial software FLUENT. Model creation and meshing were performed using the ANSYS 12.1 software package. A full-length model of one of the nine channels was used for comparison to the experiment. An inlet plenum was included in the model to improve solution convergence by buffering pressure oscillations and to simulate actual experimental conditions. All fluid properties were calculated using the NIST Real-Gas model for carbon dioxide, which utilizes highly accurate equations of state for all of the fluid properties of interest (μ , ρ , μ , and μ). The wall temperatures of the fluid channel were set from experimentally-derived values by performing conductance calculations from the thermocouple locations to the wall surface. Mass flow rate, inlet temperature and outlet pressure were matched experimentally measured values.

Modeling of turbulence in the computational fluid dynamics simulation was performed using the Shear Stress Transport (SST) k- ω model. The SST k- ω model uses two additional equations when solving the continuity, momentum, and energy equations. The two extra equations model k, which is turbulent kinetic energy, and ω , which is the specific dissipation rate of that energy. The SST version differs from the standard k- ω model by gradually varying between the k- ω model near the wall and the k- ε model far from the wall. The SST version also contains different modeling constants and extra terms to account for the blending of the k- ε and k- ω models. The

SST $k-\omega$ formulation was chosen because it was shown that a fully resolved boundary layer combined with the SST $k-\omega$ model provided the most accurate results when compared to experiment. While the $k-\varepsilon$ and $k-\omega$ models provided similar heat transfer results, the pressure drop across the channel was underestimated by around 30% when using the $k-\varepsilon$ model. Several variants of the $k-\varepsilon$ and $k-\omega$ models were tested, including both the $k-\varepsilon$ standard wall function and enhanced wall treatment models. The Figure 6 shows the comparison between data and model.

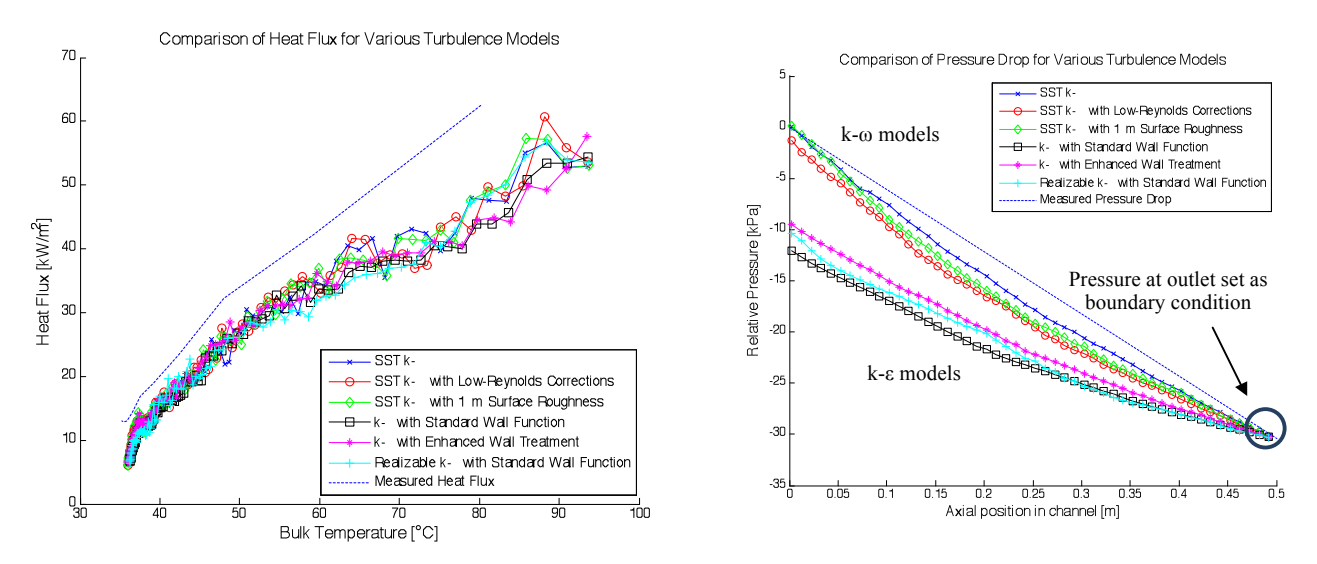


Figure 6. Comparisons of various turbulence models against experiment for heat flux and pressure drop. (Left) All turbulence models give similar heat transfer values. (Right) The SST k-ω model provides very accurate pressure drop results, while the k-ε models underestimate pressure drop by around 30%. Note that pressure drops are all normalized to the same outlet pressure.

3.0 Current Observations and Future Work

A large database has been developed for in supercritical water at UW-Madison. These tests along with the associated test facility have been scaled in preparation for conducting similar experiments in supercritical carbon dioxide. The planned experiments will use the same test section geometry and much of the same measurement equipment and techniques used in the SCW tests to allow for direct comparison of the heat transfer results, which will be used as a primary indicator of scaling law performance. As a secondary indicator, the computational fluid dynamics software FLUENT was used to compare agreement between fluid flow behaviour in select representative scaled SCW – SCO₂ case pairs. The excellent agreement seen between the predictions for the two fluids, coupled with the previously seen agreement with measured data in SCW, lend credibility to the scaling law. If the same good agreement with experimental data in SCO₂ is later found, as is expected, then the scaling law will be soundly verified. SCO₂ could then be used as a substitute fluid in experiments relating to the SCWR, which would greatly broaden the scope of possible experiments by reducing both the technical challenge and overall cost of such experiments. The one area where such an approach has been found to be deficient is when heat transfer deterioration is observed. This is still an active area of research for supercritical fluids under certain boundary conditions.

For cooling of supercritical fluids under heat exchanger conditions, heat fluxes and pressure drop data for SCO₂ were compared to CFD calculated values. It was found that the CFD predictions

for heat flux were in agreement, averaged about 5 to 25% below measured values. The pressure drops were found to be in good agreement, with about a 10% over-prediction for high mass flux cases and a 10% under-prediction for low mass flux cases. A parametric study of the pressure drop versus the corner radius was also performed, and it was found that pressure drop had a strong dependence on the corner radius. Such results suggest CFD tools are useful for design.

Acknowledgements

Support for this work was provided through the U.S. Department of Energy as well as industrial sponsors. The author wants to acknowledge the work of Research Professors, Drs. Anderson and Sridharan and UW grad students (M.Carlson, A.Kruizenga, J.Licht, E.Van Abel, S. Zwolinski).

References

- 1. DoE, "Technology Roadmap for Generation IV Nuclear Energy Systems", (March 2003).
- 2. Westinghouse Corp, "AP1000 Design Control Document", Revision 17, (October 2008).
- 3. General Electric Hitachi, "ESBWR Design Control Document", Revision 6, (August 2009).
- 4. Oka, Y, Koshizuka, J., "Concept of Once –Through cycle supercritical pressure light water cooled Reactors", November 6-8, 2002, Tokyo, Japan.
- 5. Carelli, M. et al "International Reactor Innovative and Secure (IRIS), a 1000 MWt (335 MWe) pressurized light-water reactor (PWR) design with an integral nuclear steam supply system", NURETH-12, Pittsburgh PA (Sept. 2007).
- 6. Reyes, J., <u>Identification of Proposed Pre-Application Topical Areas for NuScale PWR</u>, <u>http://www.nuscalepower.com/</u> (July, 2008).
- 7. Ball, S.J., "Next Generation Nuclear Plant GAP Report", ORNL/TM-2007/228 (July 2008).
- 8. Chang, Y. et al, "Advanced Burner Test Reactor Preconceptual Design Report", ANL-AFCI-173, Argonne National Lab (Sept 2006).
- 9. Ingersoll, D.T., <u>"Status of Physics and Safety Analyses for the Liquid-Salt-Cooled Very High-Temperature Reactor (LS-VHTR)"</u>, ORNL/TM-2005/218 (December 2005).
- 10. Sridharan, K., Anderson, M. "Molten Salt Heat Transport Loop: Materials Corrosion and Heat Transfer Phenomena", UW-Madison Technical Report, DOE/ID/14675 (Sept. 2008).
- 11. J. Licht, M. Anderson, M. Corradini, "Heat Transfer and Fluid Flow Characteristics in Supercritical Water", <u>Journal of Heat Transfer-Transactions of ASME</u>, V131, No.7 (July 2009).
- 12. S. Zwolinski, M. Anderson, J. Licht, M. Corradini, "Evaluation of Fluid-To-Fluid Scaling Method For Water And Carbon Dioxide At Supercritical Pressure", Proceedings of 5th Intl. Symposium for SCWR (ISSCWR-5) British Columbia, Canada (March 2011).
- 13. A. Kruizenga et al "Heat Transfer of Supercritical Carbon Dioxide in Printed Circuit Heat Exchanger Geometries", Proc. of 14th Int'l. Heat Transfer Conference, Wash. DC (August 2010).
- 14. M. Carlson, M. Anderson, A. Kruizenga, M. Corradini, "Measurements of Heat Transfer and Pressure Drop Characteristics of SCO2 Flowing in Zig-Zag Printed Circuit Heat Exchanger Channels", Proc. of Supercritical CO₂ Power Cycle Symposium, Boulder CO (May 2011).
- 15. E. Van Abel, M. Anderson, M. Corradini, "Numerical Investigation of Pressure Drop and Local Heat Transfer of Supercritical CO₂ in Printed Circuit Heat Exchangers", Proc. of Supercritical CO₂ Power Cycle Symposium, Boulder CO (May 2011).